

AN OFDM DESIGN FOR UNDERWATER ACOUSTIC CHANNELS WITH DOPPLER SPREAD

Sean Mason¹, Christian Berger¹, Shengli Zhou¹, Keenan Ball², Lee Freitag², and Peter Willett¹

¹Dept. of Elec. and Comp. Engr., University of Connecticut, Storrs, CT, 06269

²Applied Ocean Physics and Engr. Dept., Woods Hole Oceanographic Institution, MA 02543

ABSTRACT

In this paper, we study the performance of orthogonal frequency division multiplexing (OFDM) over underwater acoustic multipath channels with different Doppler scales on different paths. We first derive an exact inter-carrier-interference (ICI) expression after incorporating the compensation of nonuniform Doppler shifts across OFDM subcarriers. Based on the assumption that the residual ICI is dominantly from immediate neighbors, we suggest a practical design that divides subcarriers into groups, where each group of eight subcarriers consists of three contiguous data subcarriers, one pilot subcarrier, and five carefully spaced null subcarriers. We use the orthogonal matching pursuit (OMP) algorithm for sparse channel estimation that identifies distinct physical paths with different Doppler scales. System performance is evaluated using data recorded from the GLINT08 and SPACE08 experiments. Relative to the receiver that ignores the residual ICI, we observe that explicitly suppressing the residual ICI induced by Doppler spread leads to improved performance for the SPACE08 data, while not for the GLINT08 data.

Index Terms— Underwater acoustic communication, OFDM, Doppler spread, sparse channel estimation

1. INTRODUCTION

Underwater acoustic (UWA) channels exhibit long delay spreads and significant Doppler effects due to sea-surface motion and internal waves [1]. In general, the signals arriving from different propagation paths will be scaled differently due to different path variation rates. However, the receiver designs of [2, 3, 4] for multicarrier modulation over UWA channels are based on the assumption that all paths have similar Doppler scales. Inter-carrier-interference (ICI) was ignored for data demodulation after proper compensation of nonuniform Doppler shifts on OFDM subcarriers [2, 3].

Explicitly accounting for ICI caused by Doppler spread could further improve the system performance. Various approaches have been pursued in e.g., [5, 6, 7] based on a basis

expansion model (BEM) for time-varying channels such that ICI is limited to neighboring subcarriers.

In this paper, we first derive an exact ICI expression for zero-padded (ZP) OFDM signals received over a UWA channel with different Doppler scales on different paths, where the effect of the two-step compensation of nonuniform Doppler shifts across OFDM subcarriers [3] is also included. We then assume that the residual ICI is limited to immediate neighbors and present a practical ZP-OFDM design that leads to decoupled low-complexity channel estimation and demodulation. Using channel outputs on and around the pilot subcarriers, the orthogonal matching pursuit (OMP) algorithm [8, 9] is used for sparse channel estimation that identifies distinct paths with different Doppler scales.

Based on data collected in the GLINT08 and SPACE08 experiments, we compare the system performance using two receivers, one explicitly considering the residual ICI due to Doppler spread, and the other of [3] that ignores residual ICI. We observe that explicitly considering the residual ICI does not improve performance in the GLINT08 data, and hence the approach in [3] is adequate for the UWA channels in this experiment. On the other hand, the performance in the SPACE08 data benefits considerably from explicitly suppressing the residual ICI, which reveals the potential of receiver design tailored for channels with large Doppler spread.

The rest of this paper is organized as follows, in Section 2 we derive our signal model, in Section 3 we present our proposed design, detailing signal design, channel estimation and data demodulation, in Sections 4 and 5 we evaluate the performance based on experimental data, and we conclude in Section 6.

2. SYSTEM MODEL

2.1. ZP-OFDM

Let T denote the symbol duration and T_g the guard interval for the zero-padded (ZP) OFDM. The total OFDM block duration is $T' = T + T_g$ and the subcarrier spacing is $1/T$. The k th subcarrier is at frequency

$$f_k = f_c + k/T, \quad k = -K/2, \dots, K/2 - 1, \quad (1)$$

S. Mason, C. R. Berger, S. Zhou, and P. Willett are supported by the ONR YIP grant N00014-07-1-0805, the NSF grant ECCS-0725562, the NSF grant CNS-0721834, and the ONR grant N00014-07-1-0429. K. Ball and L. Freitag are supported by the ONR grant N00014-07-1-0229.

where f_c is the carrier frequency and K subcarriers are used so that the bandwidth is $B = K/T$. Let $s[k]$ denote the information symbol to be transmitted on the k th subcarrier. The non-overlapping sets of active subcarriers \mathcal{S}_A and null subcarriers \mathcal{S}_N satisfy $\mathcal{S}_A \cup \mathcal{S}_N = \{-K/2, \dots, K/2 - 1\}$. The transmitted signal in passband is given by

$$\tilde{x}(t) = \text{Re} \left\{ \left[\sum_{k \in \mathcal{S}_A} s[k] e^{j2\pi \frac{k}{T} t} q(t) \right] e^{j2\pi f_c t} \right\}, \quad t \in [0, T + T_g], \quad (2)$$

where $q(t)$ describes the zero-padding operation, i.e.,

$$q(t) = \begin{cases} 1 & t \in [0, T], \\ 0 & \text{otherwise.} \end{cases} \quad (3)$$

2.2. Channel Model

The time-varying UWA channel can be described as

$$c(\tau, t) = \sum_p A_p(t) \delta(\tau - \tau_p(t)). \quad (4)$$

Within a block of interest, each path delay can be associated with one Doppler scale factor as,

$$\tau_p(t) = \tau_p - a_p t, \quad (5)$$

and the path amplitudes are assumed constant within one OFDM block $A_p(t) \approx A_p$. Furthermore we assume that the UWA channel can be well approximated by N_p dominant discrete paths. Hence, the channel model can be simplified to

$$c(\tau, t) = \sum_{p=1}^{N_p} A_p \delta(\tau - [\tau_p - a_p t]). \quad (6)$$

Due to the adopted channel model, the received passband signal is

$$\tilde{y}(t) = \text{Re} \left\{ \sum_{p=1}^{N_p} \left[\sum_{k \in \mathcal{S}_A} s[k] e^{j2\pi \frac{k}{T} (t + a_p t - \tau_p)} \times q(t + a_p t - \tau_p) \right] A_p e^{j2\pi f_c (t + a_p t - \tau_p)} \right\} + \tilde{n}(t), \quad (7)$$

where $\tilde{n}(t)$ is the additive noise.

2.3. Receiver Processing

A two-step approach to mitigating the channel Doppler effect was proposed in [3].

1. The first step is to resample $\tilde{y}(t)$ in the passband with a resampling factor \hat{a} , leading to

$$\tilde{z}(t) = \tilde{y} \left(\frac{t}{1 + \hat{a}} \right). \quad (8)$$

2. The second step is to perform fine Doppler shift compensation on $z(t)$ to obtain $z(t) e^{-j2\pi \epsilon t}$, where ϵ is the estimated Doppler shift. The energy on null subcarriers is used to search for the best estimate of ϵ [3].

To simplify notation, we define the new residual Doppler rates and scaled delays

$$1 + b_p = 1 + \left(\frac{a_p - \hat{a}}{1 + \hat{a}} \right) = \frac{1 + a_p}{1 + \hat{a}}, \quad (9)$$

$$\tau'_p = \frac{\tau_p}{1 + b_p}. \quad (10)$$

Converting to baseband, we obtain $z(t)$

$$z(t) = \sum_{p=1}^{N_p} e^{j2\pi b_p f_c t} \sum_{k \in \mathcal{S}_A} s[k] e^{j2\pi (1+b_p) \frac{k}{T} t} \times [A_p e^{-j2\pi f_k \tau_p} q((1+b_p)(t - \tau'_p))] + n(t). \quad (11)$$

Performing ZP-OFDM demodulation, the output z_m on the m th subchannel is

$$z_m = \frac{1}{T} \int_0^{T+T_g} z(t) e^{-j2\pi \epsilon t} e^{-j2\pi \frac{m}{T} t} dt. \quad (12)$$

Plugging in $z(t)$ and carrying out the integration, we simplify z_m to

$$z_m = \sum_{p=1}^{N_p} A_p e^{-j2\pi (f_m + \epsilon) \tau'_p} \sum_{k \in \mathcal{S}_A} \varrho_{m,k}^{(p)} s[k] + v_m, \quad (13)$$

where v_m is the additive noise and

$$\varrho_{m,k}^{(p)} = \frac{\sin(\pi \beta_{m,k}^{(p)} T)}{\pi \beta_{m,k}^{(p)} T} e^{j\pi \beta_{m,k}^{(p)} T}, \quad (14)$$

$$\beta_{m,k}^{(p)} = (k - m) \frac{1}{T} + \frac{b_p f_m - \epsilon}{1 + b_p}. \quad (15)$$

Define a $K \times K$ mixing matrix:

$$[\mathbf{H}]_{m,k} = \sum_{p=1}^{N_p} A_p e^{-j2\pi (f_m + \epsilon) \tau'_p} \varrho_{m,k}^{(p)}, \quad (16)$$

a stacked received vector \mathbf{z} , data vector \mathbf{s} , and noise vector \mathbf{v} ; with this we can write the following input-output equation:

$$\mathbf{z} = \mathbf{H} \mathbf{s} + \mathbf{v}. \quad (17)$$

In case of no Doppler effects, \mathbf{H} is a diagonal matrix. When all the paths have similar Doppler scales, proper choices of \hat{a} and ϵ can render \mathbf{H} close to diagonal, which is the rational for the receiver design in [3].

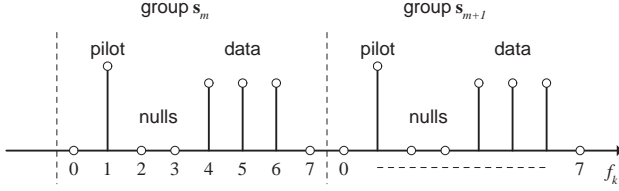


Fig. 1. The proposed OFDM subcarrier allocation

3. PROPOSED DESIGN

3.1. Signal Design

If the residual Doppler scales after the initial two-step Doppler compensation are small, i.e., $b_p f_m - \epsilon \ll 1/T, \forall m$, the off-diagonal elements of \mathbf{H} will be small. This can include larger Doppler effects, as long as the Doppler spread is small:

$$|\rho_{m,m+l}^{(p)}| \approx \left| \frac{\sin(\pi(b_p f_m T - \epsilon))}{\pi l} \right| \approx \left| \frac{(b_p f_m T - \epsilon)}{l} \right|, \forall l \neq 0, \quad (18)$$

We see that for small residual Doppler scales, from $l = 1$ to $l = 2$ there is a 3 dB amplitude drop in the coefficients. Accordingly, we choose to approximate \mathbf{H} as a tridiagonal matrix,

$$\mathbf{H} \approx \begin{bmatrix} H_{1,1} & H_{1,2} & 0 & \cdots & 0 \\ H_{2,1} & H_{2,2} & \ddots & & \vdots \\ 0 & \ddots & \ddots & & 0 \\ \vdots & & & \ddots & H_{K-1,K} \\ 0 & \cdots & 0 & H_{K,K-1} & H_{K,K} \end{bmatrix}. \quad (19)$$

To separate channel estimation and data demodulation, we suggest a simple design that places two zero subcarriers between pilots and data, see Fig. 1. We therefore define the transmit vector \mathbf{s} to consist of $M = K/8$ groups, $\mathbf{s} = [\mathbf{s}_1^T, \dots, \mathbf{s}_M^T]^T$, where each group consists of one pilot p_m and three data symbols $\mathbf{d}_m = [d_{m,1}, d_{m,2}, d_{m,3}]^T$,

$$\mathbf{s}_m = [0 \quad p_m \quad \mathbf{0}_{1 \times 2} \quad \mathbf{d}_m^T \quad 0]^T. \quad (20)$$

Note that some groups on the edges of OFDM band could be turned off.

3.2. Channel Estimation

Since every eighth subcarrier is a pilot we define the index of all pilots as $\{i_m\} = \{8 \cdot (m - 1) + 1\}$ for $m = 1, \dots, M$. Also we define the index of observations next to the pilots as $i_m^\pm = i_m \pm 1$. Based on the measurements $\{z_{i_m}, z_{i_m^+}, z_{i_m^-}\}$ on and around the pilot subcarriers, we estimate the channel paths using orthogonal matching pursuit (OMP) [8, 9]. Our implementation is mostly similar to [8], as it considers multiple Doppler scales but for single carrier transmissions.

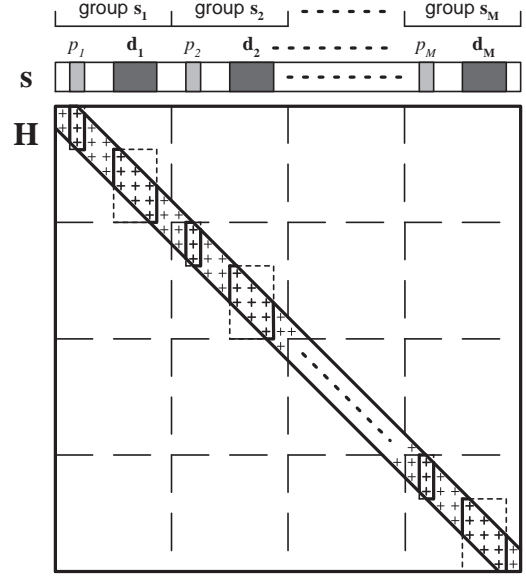


Fig. 2. Due to null subcarriers between pilots and data symbols, \mathbf{H} can be decomposed into a block-diagonal structure.

In a nutshell, based on the assumption that there is one arrival p , with a delay τ'_p and residual Doppler scale b_p , we can calculate what the received values $z_{i_m}, z_{i_m^+}, z_{i_m^-}$ would look like, see (13), and use it to calculate a correlation metric. This is performed for a grid of potential (τ'_p, b_p) and the highest value is chosen as the first path. This way, the signal is constructed as an iterative superposition of a number of discrete paths, until the fitting error in relation to the observations falls below a threshold.

3.3. Data Demodulation

Although K is large, e.g., $K = 1024$ in [3], equalization of (17) is easily possible due to the chosen design. We define the reduced channel matrix \mathbf{H}_d as the matrix \mathbf{H} using only the columns corresponding to data symbols $\mathbf{d} = [\mathbf{d}_1, \dots, \mathbf{d}_M]$:

$$\mathbf{H}_d = \begin{bmatrix} \mathbf{H}_1 & & \mathbf{0} \\ & \ddots & \\ \mathbf{0} & & \mathbf{H}_M \end{bmatrix} \quad (21)$$

The matrix \mathbf{H}_d is a block diagonal matrix consisting of M non-zero 5×3 matrices on the diagonal and zeros otherwise, see Fig. 2.

Due to the matrix model in (17), the least-squares estimates of the data symbols are simply attained using the pseudo-inverse of the estimated channel matrix,

$$\hat{\mathbf{d}} = (\hat{\mathbf{H}}_d^H \hat{\mathbf{H}}_d)^{-1} \hat{\mathbf{H}}_d^H \mathbf{z}, \quad (22)$$

Inverting $\hat{\mathbf{H}}_d^H \hat{\mathbf{H}}_d$ amounts to M parallel inversions of 3×3 matrices due to the block diagonal structure.

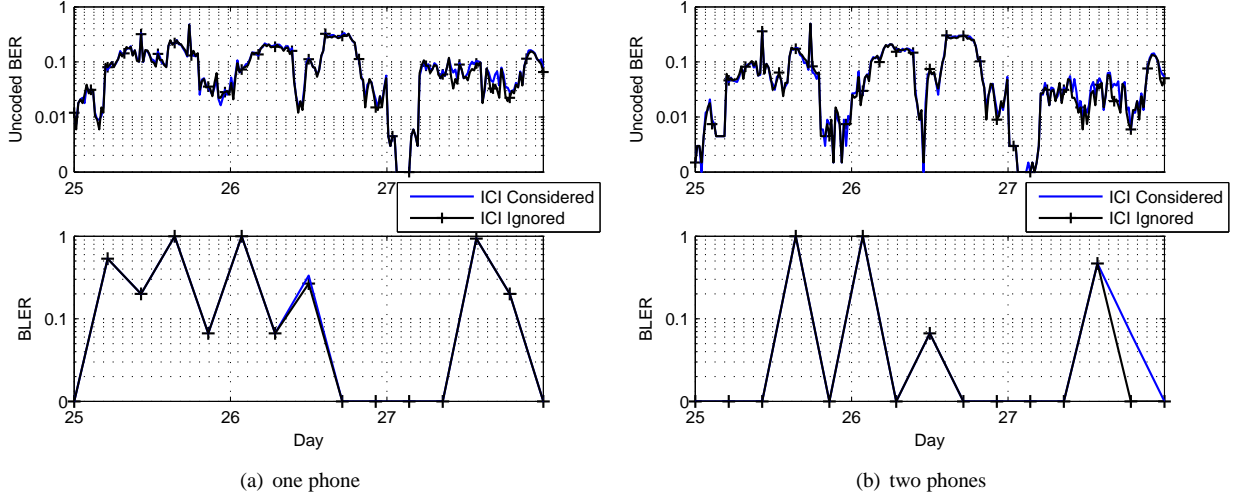


Fig. 3. Performance results for the GLINT08 data, QPSK.

4. EXPERIMENTAL RESULTS: GLINT08

Data from the GLINT experiment was collected from a drifting transmitter ship (moving at a speed from anywhere between 0.5 and 2 knots) positioned on an average distance of 1 km from the receiver, in the area around Pianosa, just south of Elba, off the coast of Italy. We focus on the data collected on three days, the 25th, 26th, and 27th of July, each of which contains five transmissions of 30 OFDM blocks per transmission (15 containing QPSK, 15 containing 16-QAM).

The center frequency was $f_c = 25$ kHz and the bandwidth was $B = 7.8125$ kHz. The sampling rate was $f_s = 250$ kHz. The number of subcarriers is $K = 1024$, which leads to subcarrier spacing of $B/K = 7.6294$ Hz and symbol duration of $T = 131.1$ ms. The guard time was set as $T_g = 25$ ms. A rate-1/2 nonbinary LDPC channel code [10] was used to map 336 information symbols to 672 coded symbols. The achieved data rates after accounting for all overheads are 2.15 kb/s and 4.30 kb/s, for QPSK and 16-QAM, respectively.

Here we compare BER results from two receivers operating upon the same data; one which employs sparse channel estimation and equalization (marked in the figures as ‘ICI considered’) and the other is the conventional receiver in [3] which ignores ICI (marked in the figures as ‘ICI ignored’). No resampling operation was necessary, and the same Doppler shift estimation is applied in both receivers.

We examine uncoded bit-error-rates (BER) and coded block-error-rates (BLER) for one and two receive elements using QPSK in the GLINT dataset; see Fig. 3. There is no noticeable difference between the two receivers. Similar observations hold true for results with 16-QAM.

For every OFDM block we measure the severity of residual ICI induced by Doppler spread through computing the ratio between the energy at the pilot-containing subcarriers to

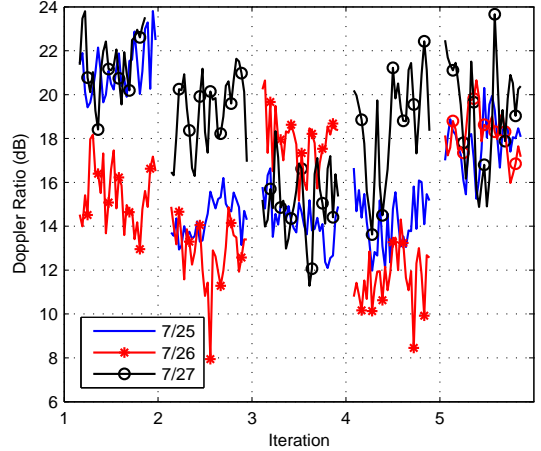


Fig. 4. The ratio of the energy measured on the pilot subcarriers to that measured at the neighboring null subcarriers; GLINT08 data

the energy at the “left and right” neighbors to those subcarriers. In Fig. 4 we observe that the energy ratio is found to be mostly between 15 and 20 dB. This shows that the residual ICI can be ignored and the low-complexity receiver in [3] is adequate for the channels in this experiment.

5. EXPERIMENTAL RESULTS: SPACE08

The SPACE08 experiment was held off the coast of Martha’s Vineyard, MA, from Oct. 14 to Nov. 1, 2008. The water depth was about 15 meters. The transmitter was about 4 meters above the sea floor, while the receiver arrays were about 3.25 meters above the sea floor. The carrier frequency was $f_c = 13$ kHz, and the bandwidth was $B = 9.76$ kHz. The

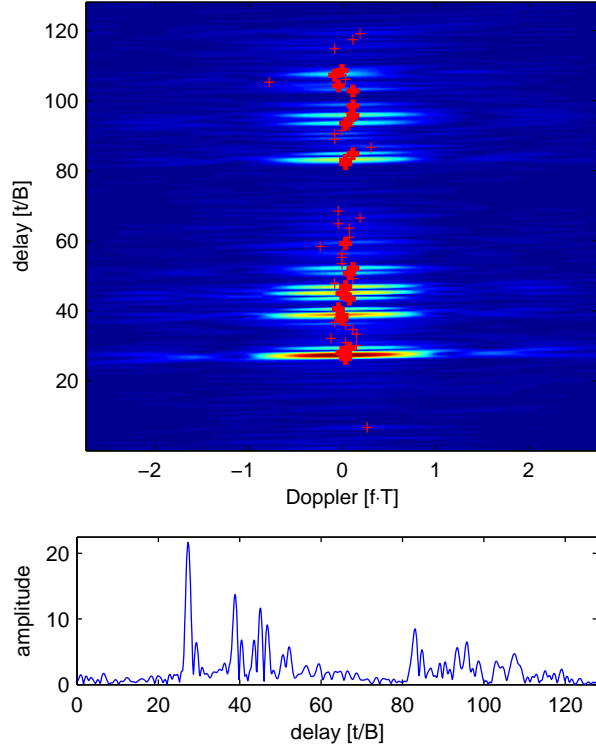


Fig. 5. Plot of (top) correlation metric of a sample SPACE08 channel used in OMP, together with chosen paths (strong amplitudes have thick marker); (bottom) correlation metric for zero Doppler in delay only.

sampling frequency was 39.0625 kHz. The number of subcarriers was $K = 1024$, which leads to a subcarrier spacing of $B/K = 9.54$ Hz and a symbol period of $T = 104.88$ ms. The guard time was set as $T_g = 24.6$ ms. A rate 1/2 non-binary LDPC channel code [10] was used that encodes 336 information symbols into 672 coded symbols. The achieved data rates were 2.60 kb/s and 5.19 kb/s, with QPSK and 16-QAM constellations, respectively.

We use 17 recorded data sets from Julian dates 290 to 298, where the transmission distance was 60 meters. A sample channel impulse response from the SPACE08 experiment is given in Fig. 5. The channel has a strong direct arrival and two large clusters of multi-path, featuring some Doppler spread. We can assume that in the delay-only view of the channel impulse response the direct arrival will be comparatively stable over time, while the two subsequent clusters will fluctuate more rapidly.

We examine the energy ratios of pilot versus neighboring null subcarriers for the SPACE08 data in Fig. 6. Those are generally smaller than the counterparts in the GLINT08 data, suggesting more severe ICI effects. In Fig. 7 we plot the performance on the QPSK modulated data with one or two receiving phones. Both receivers accomplish error free decoding, but in the uncoded BER we observe some improvement

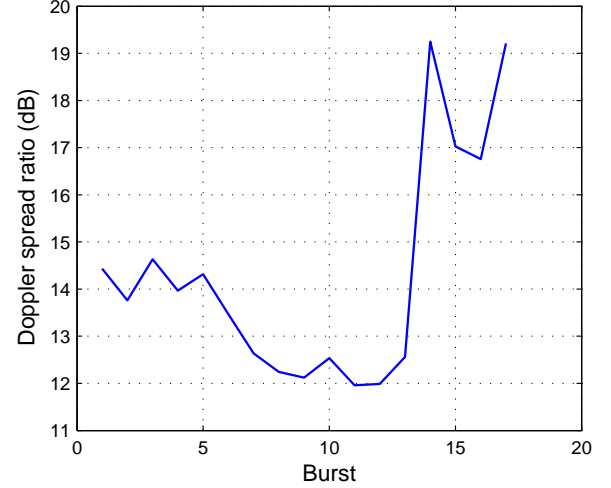


Fig. 6. The ratio of the energy measured on the pilot subcarriers to that measured at the neighboring null subcarriers; SPACE08 data

using the receiver explicitly suppressing the residual ICI.

When dealing with the 16-QAM data of the SPACE08 experiment, we use at least two receiving phones to achieve reasonable performance. While the uncoded BER only shows a typical small improvement for both cases, we see a considerable improvement in the BLER for the receiver explicitly considering the residual ICI, as shown in Fig. 8.

6. CONCLUSION

We derived an exact ICI expression after Doppler shift compensation on the received ZP-OFDM signals over a time-varying multi-path channel with different Doppler scales on different paths. To mitigate the residual ICI, we suggested a practical design which allows for decoupled block-by-block channel estimation and data demodulation. We compared the performance of a receiver design explicitly considering ICI based on a tridiagonal channel mixing matrix with that of a receiver design ignoring the residual ICI. Performance evaluation was based on data recorded from GLINT08 and SPACE08 experiments. We found that the receiver explicitly suppressing the residual ICI does not lead to noticeable improvement for the GLINT data. On the other hand, the SPACE08 data showed considerable performance improvement, often allowing successful decoding with fewer phones.

Acknowledgement

We thank Dr. James Preisig and his team for conducting the SPACE08 experiment.

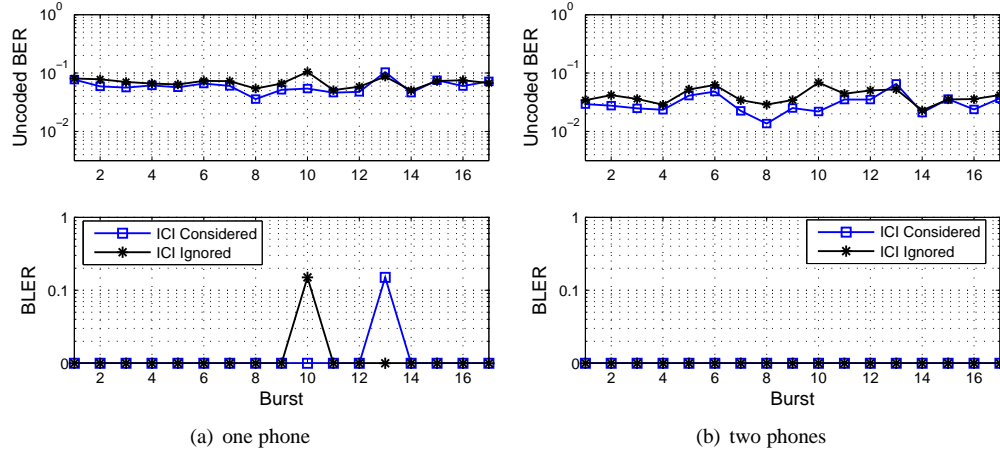


Fig. 7. Performance results for the SPACE08 data, QPSK.

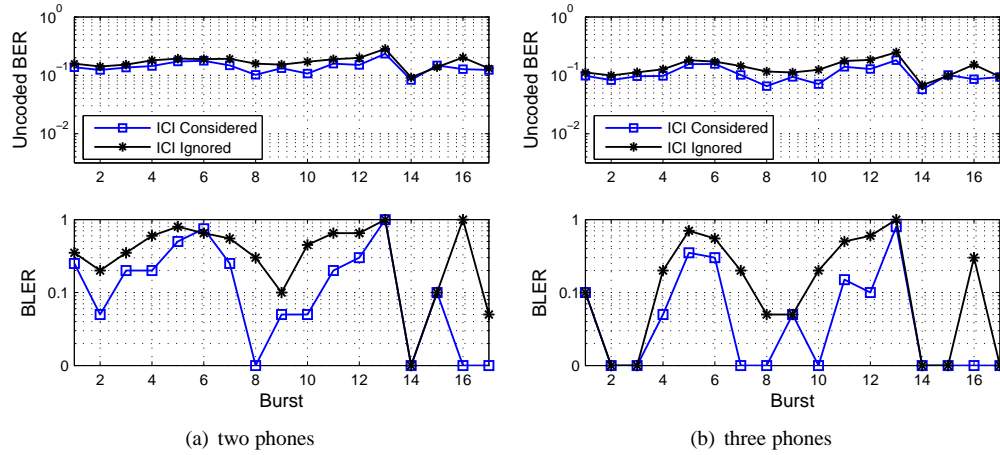


Fig. 8. Performance results for the SPACE08 data, 16-QAM.

7. REFERENCES

- [1] T. H. Eggen, A. B. Baggeroer, and J. C. Preisig, "Communication over Doppler spread channels. Part I: Channel and receiver presentation," *IEEE J. Ocean. Eng.*, vol. 25, no. 1, pp. 62–71, Jan. 2000.
- [2] M. Stojanovic, "Low complexity OFDM detector for underwater channels," in *Proc. of MTS/IEEE OCEANS conference*, Boston, MA, Sept. 18–21, 2006.
- [3] B. Li, S. Zhou, M. Stojanovic, L. Freitag, and P. Willett, "Multicarrier communication over underwater acoustic channels with nonuniform Doppler shifts," *IEEE J. Ocean. Eng.*, vol. 33, no. 2, Apr. 2008.
- [4] S. Mason, C. R. Berger, S. Zhou, and P. Willett, "Detection, synchronization, and Doppler scale estimation with multicarrier waveforms in underwater acoustic communication," *IEEE J. Select. Areas Commun.*, vol. 26, no. 9, Dec. 2008.
- [5] S.-J. Hwang and P. Schniter, "Efficient communication over highly spread underwater acoustic channels," in *Proc. of the ACM Intl. Workshop on Underwater Networks (WUWNet)*, Montréal, Québec, Sep. 2007.
- [6] F. Qu and L. Yang, "Basis expansion model for underwater acoustic channels?" in *Proc. of MTS/IEEE OCEANS Conf.*, Québec City, Québec, Sep. 2008.
- [7] G. Leus, P. van Walree, J. Boschma, C. Fanciullacci, H. Gerritsen, and P. Tusoni, "Covert underwater communications with multiband OFDM," in *Proc. of MTS/IEEE OCEANS Conf.*, Québec City, Québec, Sep. 2008.
- [8] W. Li and J. C. Preisig, "Estimation of rapidly time-varying sparse channels," *IEEE J. Ocean. Eng.*, vol. 32, no. 4, pp. 927–939, Oct. 2007.
- [9] T. Kang and R. A. Iltis, "Matching pursuits channel estimation for an underwater acoustic OFDM modem," in *Proc. of Intl. Conf. on Acoustics, Speech and Signal Proc.*, Las Vegas, NV, Apr. 2008, pp. 5296–5299.
- [10] J. Huang, S. Zhou, and P. Willett, "Nonbinary LDPC coding for multicarrier underwater acoustic communication," *IEEE J. Select. Areas Commun.*, vol. 26, no. 9, Dec. 2008.